Dalton Transactions

Accepted Manuscript

ROYAL SOCIETY OF CHEMISTRY

www.rsc.org/dalton

Cite this: DOI: 10.1039/c0xx00000x

www.rsc.org/xxxxxx

ARTICLE TYPE

Structural Variability, Topological Analysis and Photocatalytic Properties of Neoteric Cd(II) Coordination Polymers Based on Semirigid Bis(Thiazolylbenzimidazole) and Different Types of Carboxylic Acid Linkers

Lu Liu, Jie Ding, Ming Li, Xiaofeng Lv, Jie Wu*, Hongwei Hou*, Yaoting Fan

Received (in XXX, XXX) Xth XXXXXXXXX 20XX, Accepted Xth XXXXXXXXX 20XX
First published on the web Xth XXXXXXXXX 20XX
DOI: 10.1039/b000000x

A series of novel Cd^{II} coordination complexes, formulated as $\{[Cd(btbb)_{0.5}(p\text{-phda})]\cdot H_2O\}_n$ (**1**), $[Cd(btbb)_{0.5}(oba)]_n$ (**2**), $\{[Cd_2(btbb)(m\text{-bdc})_2(H_2O)]\cdot 2H_2O\}_n$ (**3**), $\{[Cd(btbb)_{0.5}(btec)_{0.5}(H_2O)]\cdot 2H_2O\}_n$ (**4**), $[Cd(btbb)_{0.5}(o\text{-bdc})]_n$ (**5**) and $\{[Cd_2(btbb)(bptc)(H_2O)]\cdot 4H_2O\}_n$ (**6**) (btbb = 1,4-bis(2-(4-thiazolyl)benzimidazole-1-ylmethyl)benzene, H_2phda = phenylenediacetic acid, H_2oba = 4,4′-oxybis(benzoic acid), *m*-H_2bdc = 1,3-benzenedicarboxylic acid, H_4btec = 1,2,4,5-benzenetetracarboxylate, *o*-H_2bdc = 1,2-benzenedicarboxylic acid, H_4bptc = 3,3′,4,4′-benzophenone tetracarboxylic acid), have been obtained by solvothermal/hydrothermal reactions for the exploration of efficient photocatalytic degradation of organic dye pollutant. Complex **1** features a 6-connected 3D *pcu* alpha-Po primitive cubic topology net with the point symbol of $4^{12}\cdot 6^3$. Interestingly, all of complexes **2**, **3** and **5** contain left- and right-handed helical chains (**2**: a 2-fold interpenetrating 3D architecture with $\{4^{12}\cdot 6^3\}$-*pcu* topology network; **3**: a (3,6)-connected net with a vertex symbol of $(4^2\cdot 5^4\cdot 6^6\cdot 7\cdot 8^2)(4\cdot 6^2)$; **5**: a (3,4)-connected 3,4L83 topology net with point symbol of $(4^2\cdot 6)(4^2\cdot 6^3\cdot 8)$). Complex **4** exhibits a (3,4)-connected 3,4T48 topology net with point symbol of $(8^4\cdot 10^2)(8\cdot 10^2)$, while complex **6** possesses a (3,5)-connected 3,5L2 topology with the point symbol of $(4^2\cdot 6)(4^2\cdot 6^7\cdot 8)$. Furthermore, the photophysical studies indicate that the relatively narrow optical energy gaps of complexes **1**–**6** (< 2.30 eV) calculated by the diffuse reflectivity spectra reflect their outstanding semiconductive nature. Since that the photocatalytic properties of complexes **1**–**6** were detailly studied, the results have demonstrated the good photocatalytic activities in methylene blue (MB) degradation reactions, especially for complexes **3**, **4** and **6** (**3**: 91.4 %, **4**: 92.7 %, **6**: 86.7 %).

Introduction

Nowadays, since many deleterious organic pollutants from industry have been released into the environment,[1-2] in particular, water, which is indispensable for the subsistence of living beings, has been grievously polluted.[3] Normally, how to acquire green, stable, penny-a-line and high-efficiency method to destroy the organic pollutant is a matter worthy of our careful consideration. To solve this problem, the semiconductor has gained more research attention as photocatalyst in the degradation of organic dye contaminants.[4] In recent years, much effort has been dedicated to exploring fresh and efficient photocatalytic materials based on metal–organic coordination polymer semiconductors with fascinating structural motifs.[5-6] Though enormous progress has been accomplished in the design and fabrication of metal–organic coordination polymers, it is still a tough job to forecast the preonunced structures of the resultant frameworks,[7] considering the truth that the crystallization process of coordination polymers is mainly influenced by various parameters, such as the coordination nature of ligand, the solvent systems, the metal atoms, the organic anions, etc.[8] Therefore, to manufacture desired crystalline product as photocatalyst in the degradation of organic dye contaminants, the crucial step is to select metal centers with appropriate geometry and connectivity as the nodes as well as meticulously designed organic spacers as linkers.

Remarkably, a number of investigations have attested that the synthetic strategy of mixed N-donor ligand and polycarboxylate

[a] *The College of Chemistry and Molecula Engineering, Zhengzhou University, Zhengzhou 450052, P. R. China* Fax: (+86) 371– 67761744 *E-mail: houhongw@zzu.edu.cn* *†Electronic supplementary information (ESI) available: X-ray crystallographic data, selected bond lengths and bond angles, additional crystal figures, powder X-ray patterns, diffuse reflectance UV-VIS-NIR spectra, and UV-vis absorption spectra for complexes* ***1*****−****6****.CCDC reference numbers: 988560–988565 for* ***1*****−****6****. For ESI and crystallographic data in CIF or other electronic format see DOI:10.1039/b000000x/*

will be a fruitful approach for the construction of diverse multidimensional structures.[9-10] Among this, the appetite are quite high for Cd(II) coordination polymers, because of their applications in photocatalysis[11], NLO materials[12] and luminescent materials[13]. As far as we can see, 1,4-bis(2-(4-thiazolyl)benzimidazole-1-ylmethyl)benzene (btbb) has been rarely mentioned as the semirigid N-donor ligand in metal–organic coordination polymer materials. btbb possesses the following characters: firstly, 2-(4-thiazolyl)benzimidazole group exhibits strong chelating coordination capacity; secondly, such groups can freely twist around two –CH_2– groups with disparate angles to product unlike conformations; thirdly, the coexistence of benzimidazolyl and thiazolyl groups enhances the whole conjugated degree, which can optimize the photophysical property of btbb ligand. Additionally, the carboxylates as multidentate O-donor coligands can demonstrate diversiform bridging/chelating modes, which are beneficial for coordinating with metal centers in the construction of metal–organic coordination polymers and also can be identified as connecting nodes or linkers building extraordinary structures and graceful topologies.[14-15] Therefore, the combination of Cd(II) and btbb and aromatic polycarboxylate species can be adopted in the effective photocatalytic degradation porcess of organic dye contaminants.

Based on the above consideration, by introducing different carboxylate coligands into the Cd(II)/btbb system, we got six Cd(II) complexes: $\{[Cd(btbb)_{0.5}(p\text{-phda})]\cdot H_2O\}_n$ (**1**), $[Cd(btbb)_{0.5}(oba)]_n$ (**2**), $\{[Cd_2(btbb)(m\text{-bdc})_2(H_2O)]\cdot 2H_2O\}_n$ (**3**), $\{[Cd(btbb)_{0.5}(btec)_{0.5}(H_2O)]\cdot 2H_2O\}_n$ (**4**), $[Cd(btbb)_{0.5}(o\text{-bdc})]_n$ (**5**) and $\{[Cd_2(btbb)(bptc)(H_2O)]\cdot 4H_2O\}_n$ (**6**) under solvothermal/hydrothermal conditions, aiming for surveying the effect of the diverse structures of polymers on their photocatalytic performances in the degradation of organic pollutants. The structures of **1**–**6** have been determined by single-crystal X-ray diffraction analyses and further characterized by infrared spectra (IR), elemental analyses, powder X-ray diffraction (PXRD). The impact of different conformational btbb and different polycarboxylates on the final networks has been discussed. Furthermore, the UV-vis spectra together with photocatalytic behaviors of **1**–**6** have also been detailly investigated.

Experimental section

Materials and Physical Measurements.

All reagents and solvents were commercially available without any further purification, except for ligand btbb, which was synthesized according to the literature.[16] The data of FT-IR spectra were calendared on a Bruker-ALPHA spectrophotometer with KBr pellets in the scale of 400−4000 cm^{-1}. Elemental analyses (C, H, and N) were carried out on a FLASH EA 1112 elemental analyzer. Powder X-ray diffraction (PXRD) patterns were recorded using the Cu $K\alpha_1$ radiation on a PANalytical X'Pert PRO diffractometer. Diffuse reflectivity spectra of the solid samples were collected with a Cary 500 spectrophotometer equipped with a 110 nm diameter integrating sphere, which were measured from 200 nm to 800 nm using barium sulfate ($BaSO_4$) as a standard with 100 % reflectance. The photocatalytic experiment for the MB degradation was investigated through a typical process. All the UV−Vis absorption spectra in solutions were illustrated by a TU-1901 double-beam UV−Vis Spectrophotometer. 50 mg powder of the designed photocatalyst and 30 % H_2O_2 (10 μL) were added into a 150 mL MB (4×10^{-5} mol L^{-1}) aqueous solution, magnetically stirred in dark for 1 h to ensure the equilibrium of adsorption/desorption. Afterwards, the solution was under the irradiation of a 500 W high-pressure mercury lamp. The solution was kept continuously stirring with the aid of a magnetic stirrer during irradiation process. At ca. 20 min intervals, 3 ml transparent sample solution were got out from the vessel and added to the 1 cm path-length quartz cell, and then analyzed by a UV-visible spectrometer. The comparative photodegradation process was also carried out under the uniform conditions without any catalyst. The typical absorption of MB at about 664 nm was chose to supervise the photocatalytic degradation process.

Synthesis

Synthesis of $\{[Cd(btbb)_{0.5}(p\text{-phda})]\cdot H_2O\}_n$ (1). A mixture of $Cd(NO_3)_2\cdot 4H_2O$ (0.1 mmol), btbb (0.05 mmol), *p*-H_2phda (0.05 mmol), EtOH (4 mL) and H_2O (6 mL) was placed in a 25 mL Teflon-lined stainless steel container at 170 °C for three days. After the mixture was cooled to room temperature at a rate of 5 °C h^{-1}, yellow block-shaped crystals suitable for X-ray diffraction were obtained with a yield of 60 % (based on Cd). Anal. Calcd for $C_{24}H_{20}CdN_3O_5S$ (%): C, 50.13; H, 3.50; N, 7.30. Found: C, 50.11; H, 3.56; N, 7.34. IR (KBr, cm^{-1}): 3443(m), 3110(w), 2931(vw), 1568(s), 1478(w), 1392(s), 931(m), 887(w), 843(w), 746(m) 630(w), 486(w).

Synthesis of $[Cd(btbb)_{0.5}(oba)]_n$ (2). A mixture of $Cd(NO_3)_2\cdot 4H_2O$ (0.2 mmol), btbb (0.1 mmol), H_2oba (0.1 mmol), and NaOH (0.2 mmol) in H_2O (9 mL) was kept in a 25 mL Teflon-lined stainless steel vessel at 170 °C for three days. After the mixture was cooled to room temperature at a rate of 5 °C h^{-1}, yellow irregular-shaped crystals suitable for X-ray diffraction were obtained with a yield of 72 % (based on Cd). Anal. Calcd for $C_{28}H_{18}CdN_3O_5S$ (%): C, 54.16; H, 2.92; N, 6.76. Found: C, 54.21; H, 2.86; N, 6.70. IR (KBr, cm^{-1}): 3440(w), 3110(w), 1594(s), 1382(s), 1226(s), 1161(m), 1097(vw), 930(w), 875(m), 852(w), 755(w), 708(m), 642(w), 524(w).

Synthesis of $\{[Cd_2(btbb)(m\text{-bdc})_2(H_2O)]\cdot 2H_2O\}_n$ (3). A mixture of $Cd(NO_3)_2\cdot 4H_2O$ (0.1 mmol), btbb (0.1 mmol), *m*-H_2bdc (0.05 mmol), EtOH (7 mL) and H_2O (3 mL) was placed in a 25 mL Teflon-lined stainless steel container. The mixture was sealed and heated at 120 °C for three days. After the mixture was cooled to ambient temperature at a rate of 5 °C h^{-1}, yellow block-shaped crystals of **3** were obtained with a yield of 48 % (based on Cd). Anal. Calcd for $C_{44}H_{34}Cd_2N_6O_{11}S_2$ (%): C, 47.53; H, 3.08; N, 7.55. Found: C, 47.59; H, 3.12; N, 7.48. IR (KBr, cm^{-1}): 3456(w), 3122(w), 3079(w), 1608(s), 1544(s), 1447(w), 1384(s), 1166(w), 1081(w), 931(m), 842(m), 748(s), 660(w), 482(w).

Synthesis of $\{[Cd(btbb)_{0.5}(btec)_{0.5}(H_2O)]\cdot 2H_2O\}_n$ (4). A mixture of $Cd(NO_3)_2\cdot 4H_2O$ (0.2 mmol), btbb (0.1 mmol), H_4btec (0.1 mmol), and NaOH (0.4 mmol) in 10 mL of CH_3OH/H_2O (v:v = 1:4) was kept in a 25 mL Teflon-lined stainless steel vessel at 160 °C for three days. After the mixture was cooled to room temperature at a rate of 5 °C h^{-1}, primrose yellow bite-size-shaped crystals suitable for X-ray diffraction were obtained with a yield of 44 % (based on Cd). Anal. Calcd for $C_{19}H_{17}CdN_3O_7S$ (%): C,

41.96; H, 3.15; N, 7.72. Found: C, 41.93; H, 3.19; N, 7.74. IR (KBr, cm^{-1}): 3411(w), 3087(w), 1590(m), 1487(w), 1370(s), 1131(w), 1011(w), 928(w), 861(w), 814(w), 748(w), 574(w), 533(w).

Synthesis of $[Cd(btbb)_{0.5}(o\text{-}bdc)]_n$ (5). A mixture of $Cd(NO_3)_2{\cdot}4H_2O$ (0.1 mmol), btbb (0.1 mmol), *o*-H_2bdc (0.05 mmol), EtOH (5 mL) and H_2O (5 mL) was placed in a 25 mL Teflon-lined stainless steel container. The mixture was sealed and heated at 180 °C for three days. After the mixture was cooled to ambient temperature at a rate of 5 °C h^{-1}, yellow irregular-shaped crystals of **5** were obtained with a yield of 57 % (based on Cd). Anal. Calcd for $C_{22}H_{14}CdN_3O_4S$ (%): C, 49.96; H, 2.66; N, 7.94. Found: C, 49.99; H, 2.65; N, 7.97. IR (KBr, cm^{-1}): 3432(w), 3106(w), 3060(w), 1610(s), 1555(s), 1478(m), 1374(s), 1315(s), 1190(w), 1082(w), 990(w), 932(s), 896(m), 830(m), 769(s), 741(s), 718(s), 694(m), 620(m), 583(m).

Synthesis of $\{[Cd_2(btbb)(bptc)(H_2O)]\cdot 4H_2O\}_n$ (6). A mixture of $Cd(NO_3)_2{\cdot}4H_2O$ (0.2 mmol), btbb (0.1 mmol), H_2bptc (0.1 mmol), and NaOH (0.4 mmol) in 10 mL of CH_3OH/H_2O (v:v = 1:4) was kept in a 25 mL Teflon-lined stainless steel vessel at 160 °C for three days. After the mixture was cooled to room temperature at a rate of 5 °C h^{-1}, yellow tip-shaped crystals suitable for X-ray diffraction were obtained with a yield of 50 % (based on Cd). Anal. Calcd. for $C_{45}H_{36}Cd_2N_6O_{14}S_2$ (%): C, 46.04; H, 3.09; N, 7.16. Found: C, 46.08; H, 3.14; N, 7.13. IR (KBr, cm^{-1}): 3406(w), 3074(w), 1587(s), 1479(m), 1376(s), 1243(s), 1160(w), 1085(m), 1029(w), 936(m), 891(vw), 833(m), 746(s), 699(w), 571(w), 479(w).

Crystal Data Collection and Refinement.

The data of the **1**–**6** were collected on a Rigaku Saturn 724 CCD diffractomer (Mo-*K*α, λ = 0.71073 Å) at temperature of 20 ± 1 °C. Absorption corrections were applied by using multi-scan program. The data were modified for Lorentz and polarization effects. The structures of complexes **1**–**6** were solved by direct methods and refined with a full-matrix least-squares technique based on F^2 with the SHELXL-97 crystallographic software package.[17] All non-H atoms were refined anisotropically except for the O11, O12 and O14 atoms of complex **6**. The solvent water molecules in **6** are a little disordered and their U(eq) values have been fixed. The hydrogen atoms were placed at calculated positions and refined as riding atoms with isotropic displacement parameters. Crystallographic crystal data and structure processing parameters for **1**–**6** are summarized in Table S1 (in the Supporting Information). Selected bond lengths and bond angles of **1**–**6** are listed in Table S2 (in the Supporting Information). Crystallographic data for **1**−**6** have been deposited at the Cambridge Crystallographic Data Centre with CCDC reference numbers 988560–988565.

Results and Discussion

X-ray Crystallography and Characterization.

Crystalline complexes **1**−**6** were synthesized by the solvothermal/hydrothermal reactions of the semirigid N-donor ligand btbb and the different O-donor coligands (carboxylates). Single-crystal X-ray diffraction analyses, infrared spectra (IR), satisfactory elemental analyses, and powder X-ray diffraction (PXRD) confirmed the identities of complexes **1**−**6**.

1 crystallizes in triclinic system with $P\bar{1}$ space group. The asymmetric unit of complex **1** consists of one Cd(II) atom, half a btbb ligand, one *p*-$phda^{2-}$ ligand and one lattice water molecule. As depicted in Figure S1, the Cd(II) atom also sits in a distorted octahedral coordination geometry with CdO_4N_2 coordination environment defined by two nitrogen atoms (N1 and N3) from one btbb ligand and four oxygen atoms (O1, O2, O3, O3A) from three different *p*-$phda^{2-}$ ligands. The Cd−O bond distances vary from 2.266(3) to 2.502(4) Å, while the Cd−N bond lengths are in the range of 2.311(3)–2.382(4) Å.

Ligand btbb (with the $N_{donor}\cdots N{-}C_{sp3}\cdots C_{sp3}$ torsion angle of 99.700 º) and *p*-$phda^{2-}$ anions (the angle of $-CH_2-$ is 108.303 º) both adopts symmetric *trans*-conformation. The two carboxylic groups of one kind of *p*-$phda^{2-}$ ligand take an uniform bidentate chelating mode. The two carboxylic groups of the other kind of *p*-$phda^{2-}$ ligand also have an uniform coordination mode, both in μ_2-η^2:η^0 fashion. The Cd(II) atom are linked by the *p*-$phda^{2-}$ ligands to generate a 2D sheet (Figure 1a) containing the centrosymmetric Cd_2 dinuclear unit linked by μ_2-O of two carboxylate groups. The four atoms (Cd−O−Cd−O) of the dinuclear unit are completely coplanar, and Cd···Cd and O···O distances are 3.639 and 2.760 Å, respectively. The sheets are pillared by ligands btbb in a *trans*-conformation via the Cd···N connections to generate a pillar layered 3D framework (Figure 1b). Visibly, the 3D framework of **1** can be described as 6-connected *pcu* alpha-Po primitive cubic topology with the point symbol of $4^{12}{\cdot}6^3$ (Figure 1c), when the Cd_2 dinuclear unit is simplified as node, and btbb and *p*-$phda^{2-}$ ligands are defined as linkers, respectively.

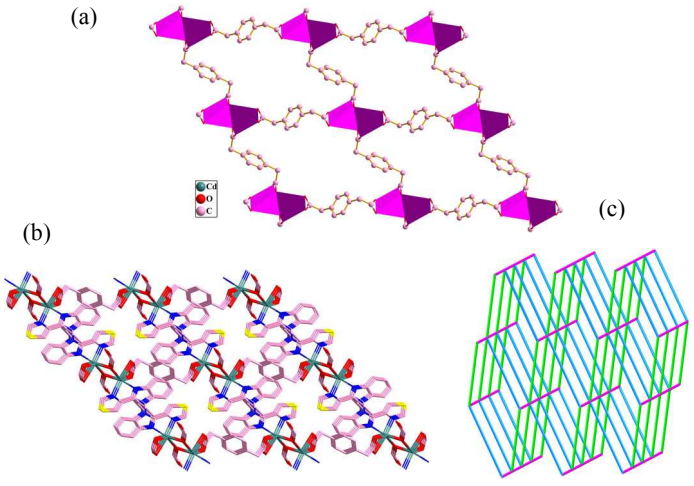

Figure 1. (a) The 2D sheet of **1** built through Cd(II) ions and *p*-$phda^{2-}$ linkers. (b) Schematic view of the 3D architecture built by 2D Cd(II)/*p*-$phda^{2-}$ layers and btbb pillars (H atoms omitted for clarity). (c) Schemetic view of the 3D topology network for **1** (bright green line: btbb; light blue line and pink line: the two kinds of *p*-$phda^{2-}$).

The asymmetric unit of complex **2** contains one Cd(II) atom, half a btbb ligand and one oba^{2-} ligand in the monoclinic space group $P2_1/c$. Depicted in Figure S2, the Cd center is seven-coordinated by five oxygen atoms (O1, O2A, O3B, O4B and O4C) belonging to four separated oba^{2-} ligands as well as two nitrogen atoms (N1

and N3) from btbb ligand to generate a pentagonal biyramid coordination geometry. The Cd–O and Cd–N bond distances lie in the ranges of 2.297(3)–2.634(4) Å and 2.350(4)–2.498(5) Å, respectively, which is well comparable with values reported.[18]

In **2**, the btbb adopts symmetrical *trans*-conformation with the $N_{donor}\cdots N{-}C_{sp3}\cdots C_{sp3}$ torsion angle of 68.606 º. The dihedral angle between two benzene rings of oba^{2-} is 77.729 º and the oba^{2-} anion connects four Cd(II) cations, where one carboxylate group takes μ_2-η^1:η^1 coordination mode, and the other carboxylate group adopts μ_2-η^2:η^1 fashion. Each pair of Cd(II) ions is bridged by such four oba^{2-} anions to yield a well-known paddle-wheel binuclear clusters $[Cd_2(COO)_4]$ with a Cd···Cd distance of 3.419 Å. The binuclear clusters are further extended by oba^{2-} anions into a 2D net (Figure 2a) with alternately arranged left- and right-handed helical chains (Figure 2b). Both the helical pitches are 14.279(3) Å corresponding to the length of *b*-axis. Parallel 2D Cd(II)/oba^{2-} nets are connected by the btbb ligands acting as pillars to form a 3D network (Figure 2c). From a topological perspective, the dinuclear unit $[Cd_2(COO)_4]$ acts as a six connected node, and complex **3** represents $\{4^{12}\cdot6^3\}$-*pcu* topology by using btbb and oba^{2-} ligands as linkers. Two identical nets are further interpenetrating with each other, resulting into the final 2-fold network (Figure 2d).

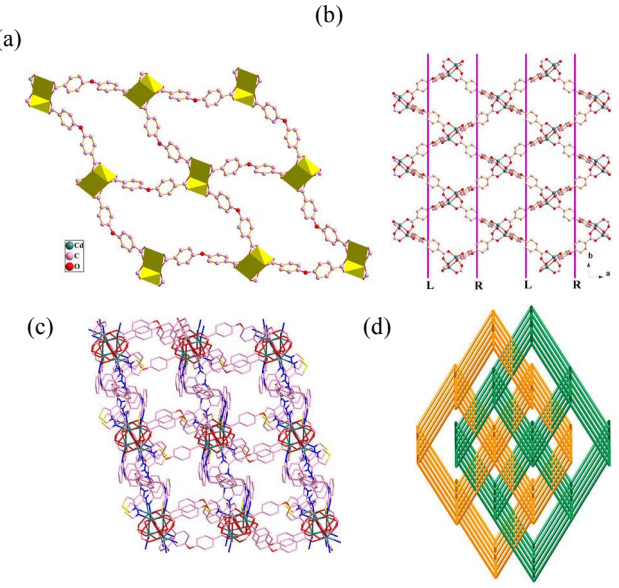

Figure 2. (a) The 2D layer of **2** constructed from Cd(II) ions and oba^{2-} anions. (b) View of the 2D Cd(II)/oba^{2-} net built by alternately left- and right-handed helical chains. (c) Schematic view of the 3D architecture built by 2D Cd(II)/oba^{2-} layers and btbb pillars in **2** (H atoms omitted for clarity). (d) Schematic representation of the 2-fold interpenetrated topology nets for **2**.

For complex **3**, it consists of two crystallographically independent Cd(II) atoms, one btbb ligand, two *m*-bdc^{2-} ligands, one coordinated water molecule and two lattice water molecules. As illustrated in Figure S3, Cd1 atom is seven-coordinated by five O atoms of carboxylate groups (O1, O2, O5, O6 and O8B) provided by three different *m*-bdc^{2-} ligands and two nitrogen atoms (N1 and N2) deriving from one btbb ligand to give a pentagonal bipyramidal coordination geometry. The distances of Cd1–N1/N2 are 2.389(5)/2.312(4) Å, while the Cd1–O bond lengths range from 2.260(4) to 2.593(5) Å. Cd2 atom is six coordinated with coordination geometry of octahedron, which is completed by three oxygen atoms (O3, O4 and O7A) originating from two different *m*-bdc^{2-} anions, one oxygen atom (O9) afforded by one coordinated water molecule and two nitrogen atoms (N4 and N5) from one btbb ligand. The distances of Cd2–N4/N5 are 2.264(4)/2.455(5) Å, while the Cd2–O bond lengths range from 2.210(5) to 2.399(5) Å.

There are two independent btbb ligands in complex **3**, both of which exhibit symmetrical *trans*-conformation. $N_{donor}\cdots N{-}C_{sp3}\cdots C_{sp3}$ torsion angles of btbb-I are 99.315 º. While $N_{donor}\cdots N{-}C_{sp3}\cdots C_{sp3}$ torsion angles of btbb-II are 84.903 º. Ligands *m*-bdc^{2-} with a angle of 120 º between two carboxylic groups of **3** take two different coordination modes. The first type (*m*-bdc^{2-}-I) is that one carboxylate group of *m*-bdc^{2-} ligand adopts a chelating bidentate mode, and the other is in a bridging bidentate mode, whereas the two carboxylate groups of the second type (*m*-bdc^{2-}-II) both adopt chelating bidentate modes. The *m*-bdc^{2-}-I anions give rise to a closed loop by coordinating to two Cd1(II) ions resulting in a Cd_2(*m*-bdc)$_2$ metallocyclic motif. The Cd_2(*m*-bdc)$_2$ units are linked by *m*-bdc^{2-}-II anions leading to a 1D double chain (Figure 3a). Notably, Cd(II) atoms are bridged by the two types of *m*-bdc^{2-} to give a coexistence of two kinds of helical chains, a left-handed chain and a right-handed helical chain, with the equal pitch of 11.485 Å corresponding to the length of *a*-axis (Figure 3b). The extension of the structure into a 3D network is also accomplished by connecting 1D double chains through two kinds of *trans*-conformational btbb ligands (Figure 3c). To further demonstrate the overall 3D structure of **3**, we can consider each Cd_2(*m*-bdc)$_2$ as a 6-connecting node, which is linked to six equivalent nodes through two Cd2 cations, two btbb ligands and two *m*-bdc^{2-}-II anions. The Cd2 cations can be considered as a 3-connected node, which is connected to three equivalent nodes through one btbb ligand, one Cd_2(*m*-bdc)$_2$ unit and one *m*-bdc^{2-}-II anion. Moreover, the btbb-I/II and *m*-bdc^{2-}I/II anions are simplified as linear linkers, separately. With further topological analysis by the *OLEX* program, the whole structure of **3** can be simplified to a (3,6)-connected net with a vertex symbol of $(4^2\cdot5^4\cdot6^6\cdot7\cdot8^2)(4\cdot6^2)$ (Figure 3d).

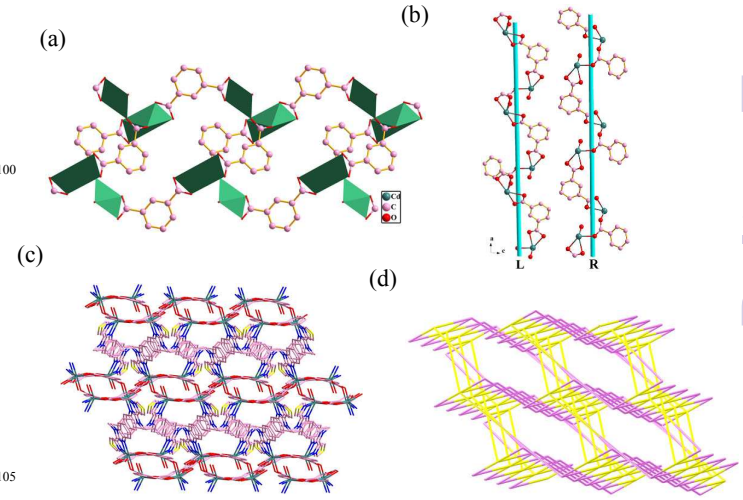

Figure 3. (a) The one-dimensional (1D) double chain of **3** fabricated from two types of Cd(II) ions and two kinds of *m*-bdc^{2-} anions. (b) View of the Cd(II)/*m*-bdc^{2-} left- and right-handed helical chains along the *b*-axis. (c) Schematic view of the 3D framework built by 2D Cd(II)/*m*-bdc^{2-} layers and btbb pillars in **3** (H atoms omitted for clarity). (d) Schemetic view of the 3D topology network with a vertex symbol of $(4^2{\cdot}5^4{\cdot}6^6{\cdot}7{\cdot}8^2)(4{\cdot}6^2)$ for **3** (yellow line: btbb; pink line: *m*-bdc^{2-}).

As illustrated in Figure S4, the asymmetric unit of complex **4** consists of one Cd(II) atom, half a btbb ligand, half a H_4btec ligand, one coordinated water molecule and two lattice water molecules. Each Cd(II) atom is six-coordinated by three carboxylate oxygen atoms (O1, O3A and O4A) from two btec^{4-} anions, two nitrogen atoms (N1 and N2) from one btbb ligand and one oxygen atom (O5) from one water molecule. The Cd–O bond distances vary from 2.223(5) to 2.490(5) Å, while the Cd–N1/N2 bond lengths are 2.450(6)/2.315(6) Å, severally. Ligand btbb adopts symmetric *trans*-conformation with a $N_{donor}\cdots N$–$C_{sp3}\cdots C_{sp3}$ torsion angle of 78.697 º. The btec^{4-} anion presents a quadridentate coordination mode, with two carboxylate groups adopting the bidentate chelate modes and two carboxylate groups showing the monodentate modes. The Cd(II) atoms are connected by btec^{4-} anions to form a 2D sheet structure (Figure 4a), which is connected by btbb ligand in a *tran*-conformation via the Cd–N connection to generate a 3D pillar-layered framework (Figure 4b). As discussed above, each btec^{4-} anion links four Cd(II) atoms, and accordingly, the btec^{4-} can be regarded as a 4-connected node. As for each Cd(II) atom, it links two btec^{4-} anions and one btbb ligand, hence, the Cd(II) atom is treated as a 3-connector. According to the simplification principle, the resulting structure of complex **4** is a binodal (3,4)-connected 3,4T48 topology net with point symbol of $(8^4{\cdot}10^2)(8{\cdot}10^2)$ (Figure 4c).

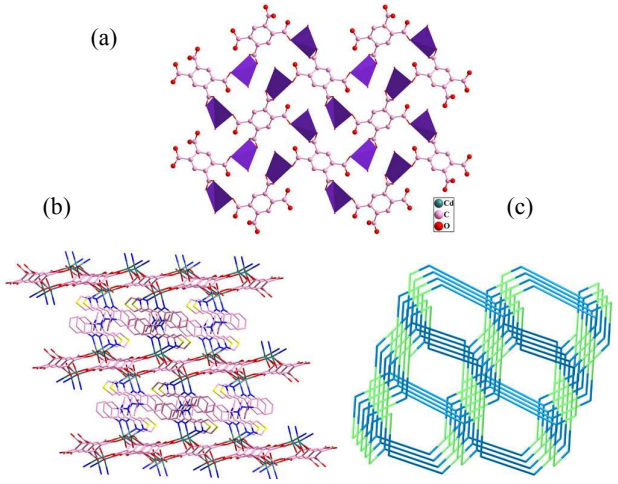

Figure 4. (a) Two-dimensional (2D) sheet generated by Cd(II) ions and btec^{4-} linkers in **4**. (b) Schematic view of the 3D framework built by 2D Cd(II)/btec^{4-} layers and btbb pillars in **4** (H atoms omitted for clarity). (c) Schemetic view of the 3D topology network with point symbol of $(8^4{\cdot}10^2)(8{\cdot}10^2)$ for **4** (light blue line: btbb).

Structural analysis indicates that complex **5** is a 2D structure with (3,4)-connected 3,4L83 topology and crystallizes in the triclinic $P\bar{1}$ space group. The asymmetric unit of **5** is composed of one crystallographically independent Cd(II) ion, half a btbb ligand, and one *o*-bdc^{2-} ligand. As shown in Figure S5, the Cd(II) ion adopts a distorted octahedral coordination environment, which is provided by two nitrogen atoms (N1, N2) from one separate btbb and four oxygen atoms (O1, O2A, O3A, O4B) from three *o*-bdc^{2-} anions. The Cd−O distances are in the range of 2.274(3)–2.323(3) Å, while the Cd−N bond length are in the range of 2.386(3)–2.431(3) Å, which are in the normal range.[18] btbb shows the symmetric *trans*-conformation with the $N_{donor}\cdots N$–$C_{sp3}\cdots C_{sp3}$ torsion angle of 81.698 º. The two carboxylic groups of each *o*-bdc^{2-} anion both adopt μ_2-η^1:η^1 coordination mode. By this way, each *o*-bdc^{2-} anion bridges three Cd(II) ions to give rise to an uniform Cd chain (Cd(II)/*o*-bdc^{2-} chain) along the *b*-axis (Figure 5a). The Cd$\cdots$Cd separation across −O−C−O− bridges are 4.359 Å and 5.183 Å, separately. Interestingly, left- and right-handed helical chains which share Cd(II) ion, were found along the *b*-axis in the Cd(II)/*o*-bdc^{2-} chain (Figure 5b). Both the helical pitches are 7.694 Å corresponding to the length of *a*-axis. The Cd(II) ions of two neighboring 1D Cd(II)/*o*-bdc^{2-} chains were connected by the *trans*-conformational btbb ligands generating the 2D sheet of **5** (Figure 5c), with a Cd$\cdots$Cd distance of 14.847 Å. As depicted in Figure 5d, topological analysis is performed on **5**. Each Cd(II) ion is encircled by four organic ligands (one btbb ligand and three *o*-bdc^{2-} ligands), and each *o*-bdc^{2-} ligand is linked to three Cd(II) ions. If the Cd(II) ion is taken as a 4-connector, the *o*-bdc^{2-} can be simplified as 3-connected and bbtb is defined as linkers, the 2D framework of **5** can be described as $(4^2{\cdot}6)(4^2{\cdot}6^3{\cdot}8)$ topology.

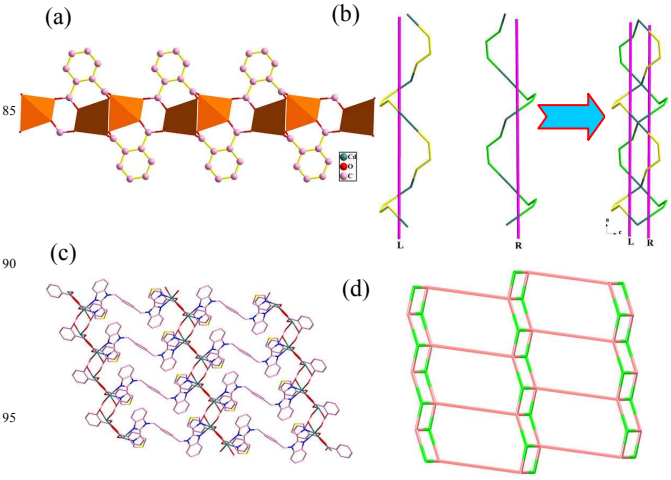

Figure 5. (a) The 1D chains built though Cd(II) ions and *o*-bdc^{2-} linkers in **5**. (b) View of the Cd(II)/*o*-bdc^{2-} left- and right-handed helical chains along the *b*-axis. (c) The 2D layer structure of **5** constructed by btbb and 1D Cd(II)/*o*-bdc^{2-} chain. (d) Schematic description of a (3,4)-connected 2D network with $(4^2{\cdot}6)(4^2{\cdot}6^3{\cdot}8)$ topology for **5** (carmine line: btbb).

At last, complex **6** exhibits a beautiful (3,5)-connected 2D network, which crystallizes in the triclinic system, space group $P\bar{1}$. Each asymmetric unit of **6** consists of two crystallographically independent Cd(II) ions, one btbb, one bptc^{4-}, one coordinated water molecule, and four guest water molecules. Figure S6 illustrates the coordination environment of the Cd(II) ions. The octahedral coordination geometry of the central Cd1 ion is completed by two N atoms (N1 and N3) of one btbb ligand, and

four O atoms (O1, O2, O5A, O7B) of three $bptc^{4-}$ anions. Cd2 ion also shows a distorted octahedral coordination geometry, which is defined by three oxygen atoms (O4D, O7C, O9C) from three $bptc^{4-}$ anions, one oxygen atom (O3) from one coordinated water molecule, and two nitrogen atoms (N5 and N6) from one btbb ligand. The distances of Cd–O/N bond are in the range of 2.250(4)–2.388(5) Å. They are reasonable to compare with those in reported works[18]. The btbb ligand adopts asymmetric *trans*-conformation with two different $N_{donor}\cdots N{-}C_{sp3}\cdots C_{sp3}$ torsion angles of 81.644 º and 102.458 º.

In **6**, the $bptc^{4-}$ anions connects five Cd(II) cations, one carboxylate group takes μ_2-η^1:η^1 coordination mode, the other carboxylate group adopts μ_1-η^1:η^1 fashion, the third shows μ_1-η^1:η^0 coordination mode, and the forth exhibits μ_2-η^2:η^0 fashion. Cd1 and Cd2E (E = 1+x, y, 1+z) ions are held together by the carboxylate O atoms to form a binuclear unit $[Cd_2(CO_2)O]$, which likes a fine bud. The Cd–Cd distance across the binuclear unit is 4.179 Å. The binuclear $[Cd_2(CO_2)O]$ units are connected by the $bptc^{4-}$ ligands resulting in a 1D double chains (Figure 6a). The 1D chains are further interlinked by btbb ligands to yield a 2D layer (Figure 6b). The bridged Cd···Cd distance along μ-btbb is 14.618 Å. From a topological perspective, each binuclear SBU is surrounded by five organic ligands (two btbb ligands and three $bptc^{4-}$ ligands), and each $bptc^{4-}$ ligand is connected to three binuclear $[Cd_2(CO_2)O]$ units. Hence, the $[Cd_2(CO_2)O]$ units can be regarded as 5-connected nodes, the $bptc^{4-}$ anions are defined as 3-connected nodes and btbb ligands are considered as linkers, respectively, the 2D framework of **6** can be represented as a 3,5L2 topology with the point symbol of $(4^2{\cdot}6)(4^2{\cdot}6^7{\cdot}8)$ (Figure 6c).

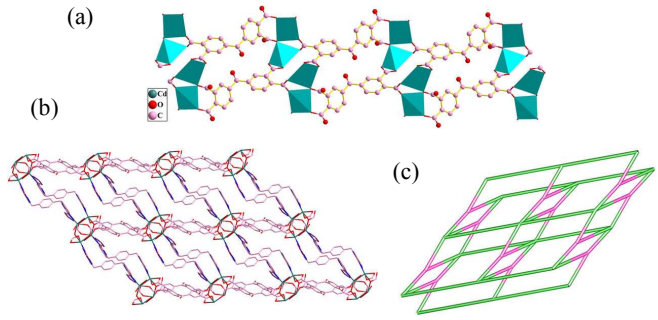

Figure 6. (a) The 1D double chains built though Cd(II) ions and $bptc^{4-}$ linkers in **6**. (b) The 2D layer structure of **6** consists of btbb and 1D Cd(II)/$bptc^{4-}$ chain. (c) Schematic representation of a (3,5)-connected topology network with a point symbol of $(4^2{\cdot}6)(4^2{\cdot}6^7{\cdot}8)$ for **6** (green line: btbb).

Effect of Btbb and Carboxylate Coligands on the Structures of Complexes 1–6

The PXRD patterns for complexes **1**–**6** are shown in the Figure S7. The diffraction peaks of experimental patterns match well with the simulated data, indicating that all of the synthesized bulk materials are consistent with the measured single crystals. As described above, the semirigid btbb ligand presents symmetric *trans*-conformation in **1**–**5**, asymmetric *trans*-conformation in **6**. The free conformations of $-(CH_2)-$ spacer greatly enrich structures of complexes **1**−**6**. In **1**, **2** or **4**, btbb serves as bridging pillar linking adjoining 2D layer, which makes them show 3D pillar-layered framework. However, in **3**, two kinds of independent btbb bridges adjacent 1D Cd(II)/*m*-bdc^{2-} chains leading to the 3D architecture of **3**. For **5** or **6**, btbb connects neighboring 1D Cd(II)/*o*-bdc^{2-} chains and 1D Cd(II)/$bptc^{4-}$ chains, respectively, yielding two 2D nets. From the structure descriptions above, the btbb utilizes its four N atoms of the 2-(4-thiazolyl)benzimidazole group to coordinate to the metal ions just like a linker. As a result, the 1D/2D structures built by metal ions and aromatic multicarboxylate ligands are connected by btbb to product 2D/3D architectures with versatile topologies.

Six different carboxylates have been chosen as coligands in synthesis process of **1**–**6**. In **1**, *p*-$phda^{2-}$ anions adopting symmetric *trans*-conformation, link two adjoining Cd(II) ions to yield a 2D layer, which is pillared by btbb to form a 3D framework with 6-connected *pcu* alpha-Po primitive cubic topology. When H_2oba is introduced into the synthetic procedure of **2**, a 2-fold interpenetrating 3D network with the point symbol of $(4^{12}{\cdot}6^3)$ are constructed. The oba^{2-} anions bridges Cd(II) ions to generate well-known paddle-wheel binuclear clusters and the binuclear clusters are further extended by oba^{2-} anions into 2D nets with alternately arranged left- and right-handed helical chains. In **3**, we select *m*-H_2bdc with a rigid spacer and an angle of 120 º between the two carboxylic groups as a coligand. The *m*-bdc^{2-}-I anions connect two Cd(II) ions resulting in a Cd_2(*m*-bdc)$_2$. The dual-core Cd_2(*m*-bdc)$_2$ units are linked by *m*-bdc^{2-}-II anions leading to the production of a 1D double chain. Besides that, the Cd(II) atoms are bridged by the two types of *m*-bdc^{2-} to afford a coexistence of left-handed and right-handed helical chain. Because of *o*-H_2bdc with an angle of 60 º between the two carboxylic groups, **5** shows the 3,4L83 topology net. The perceivably structural differences of **3** and **5** manifest that diverse coordination modes of carboxylate groups and different angles between the two carboxylic groups play important roles in the fabrication of complexes. In the presence of H_4btec adopting a quadridentate coordination mode, the 3D framework with 3,4T48 topology net of **4** is achieved. In **6**, the introduction of "V" shape ligand H_4bptc bring about the formation of the 2D 3,5L2 topology net. The four carboxylate groups of the $bptc^{4-}$ anions connect five adjacent Cd(II) ions resulting in a 1D double chain. These results make clear that various carboxylate coligands exert a profound influence on the formation of holistic structures of the ultima complexes and the situation further testifies that a mixed ligand strategy is conducive to the building of complexes with different structures and topologies.

Photophysical Properties and Optical Band Gaps.

As well-known, the photophysical property studies of the N-donor ligand btbb, the O-donor ligands (*p*-H_2phda, H_2oba, *m*-H_2bdc, H_4btec, *o*-H_2bdc, H_4bptc) and the complexes **1**–**6** in solid state at room temperature are favorable to preparatorily select the efficient photocatalyst systems for the further photochemical experiments to decompose the organic dye methylene blue (MB). As depicted in Figure S8, diffuse-reflectance UV-vis spectrum of the ligand btbb shows two intense absorption bands (λ_{max} = 241 nm, 5.16 eV; λ_{max} = 323 nm, 3.85 eV) and one medium absorption band (λ_{max} = 434 nm, 2.86 eV) in the range of 210–500 nm, which are ascribed to the typical $\pi\rightarrow\pi^*$ transitions.[19]

Moreover, the UV-vis absorption spectra of six aromatic polycarboxylates indicate most intense absorption bands with

maxima less than 310 nm (4.01 eV), such as 261 and 304 nm for *p*-H_2phda, 243 and 294 nm for H_2oba, 248 and 298 nm for *m*-H_2bdc, 244 and 304 nm for H_4btec, and 244 and 300 nm for *o*-H_2bdc; except for H_4bptc, which displays one broad band at 287 nm and one shoulder band at 385 nm in the scale of 210–450 nm. Due to the relevant literatures[20-21], all the absorption bands are assigned to the $\pi\rightarrow\pi^*$ transitions of the aromatic rings in the free ligands, respectively. Noticeably, the lowest energy absorption bands of btbb ligand are lower than that of all the aromatic carboxylate ligands in the energy level, which indicates that btbb ligand might have more influence than the lowest energy absorption band of the aromatic carboxylate ligands through the coordination with the metal ion. However, because the lowest energy absorption band of H_4bptc (λ_{max} = 385 nm, 3.22 eV) is close to that of btbb (λ_{max} = 434 nm, 2.86 eV), the lowest energy absorption band of complex **6** will be affected by the synergy of N-donor ligand btbb and O-donor H_4bptc.

As we expected, all the complexes **1**–**6** show the similar lowest energy absorption bands with maxima more than 450 nm (2.76 eV, Figure S9), which can be mainly owing to the coordination of btbb to the Cd(II) ion decreasing the energy gap of the intraligand (IL, $\pi\rightarrow\pi^*$) transition in nature. Importantly, as reported in the literature,[22] the optical band gap (Eg) of the photocatalyst was one main factor for the decomposition efficiency of the organic dyes. Herein, in order to investigate the semiconductor properties of complexes **1**–**6**, the measurements of their diffuse reflectivity were executed to acquire their band gaps (Eg). The band gap E_g were defined as the intersection point between the energy axis and the line extrapolated from the linear portion of the adsorption edge in a plot of Kubelka−Munk function F *versus* energy E. Kubelka−Munk function, $F = (1-R)^2/2R$, was transformed from the recorded diffuse reflectance data, where R is the reflectance of an infinitely thick layer at any given wavelength (The F against E plots are revealed in Figure S10) [23], and the Eg values evaluated from the steep absorption edge are 2.20 eV for **1**, 2.17 eV for **2**, 2.14 eV for **3**, 2.08 eV for **4**, 2.18 eV for **5**, 2.09 eV for **6**, respectively, which demonstrates that complexes **1**–**6** are underlying semiconductive materials[24] and can serve as photocatalysts.[6,25]

Photocatalytic Activity.

To examine the photocatalytic activity of complexes **1**–**6**, methylene blue (MB), which is hard to decompose in wastewater, was selected as the model dye contaminant to appraise the photocatalytic effectiveness in the purification of wastewater. In addition, each sample solution was exposed to the stable and quantitative irradiation from a 500 W high pressure mercury vapor lamp at a distance of 5 cm between the liquid surface and the lamp. As illustrated in Figure 7, the absorption peaks of MB decreased patently following the reaction time in the presence of **1**–**6**.

Besides that, the changes in the C_t/C_0 plot of MB solution against irradiation time are painted in Figure 8 (wherein C_0 is the initial concentration of the MB solution and C_t is the concentration of the MB at any given time t). The calculation results embody that the photocatalytic activities increase from 16.8 % (control experiment without any catalyst) to 66.7 % for **1**, 23.1 % for **2**, 91.4 % for **3**, 92.7 % for **4**, 76.9 % for **5** and 86.7 % for **6** after 140 min of irradiation. In the presence of catalyst, the distinctly increased photocatalytic decomposition rate indicates that complexes **1**–**6** are energetic for the degradation of MB under UV irradiation and probably possess potential photocatalytic application in the decomposition of some organic dyes. After photocatalysis, complexes **1**–**6** were filtered and observed under an optical microscope. The crystal shape of **1**–**6** did not change, manifesting that they are stable in the degradation of MB. Thus, this experiment does not introduce the new pollutant, Cd ion, in the water.

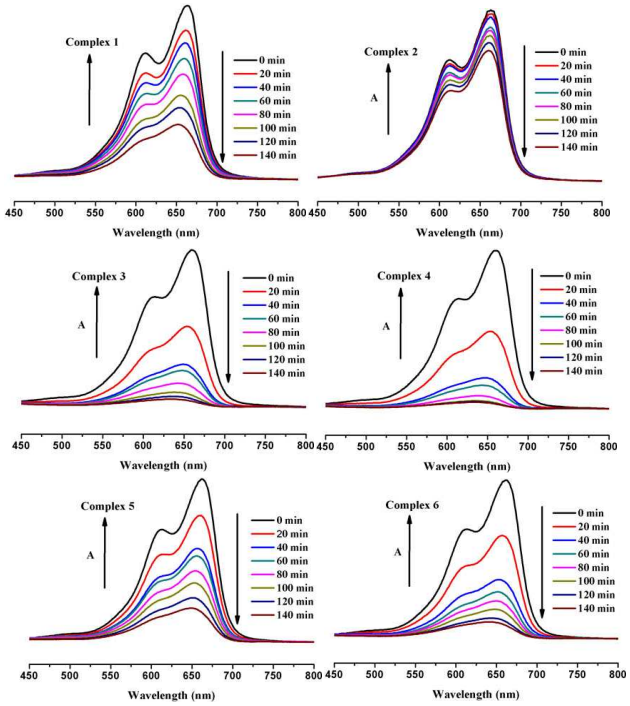

Figure 7. Absorption spectra of the MB solution during the decomposition reaction under UV light irradiation with the presence of complexes **1**–**6**.

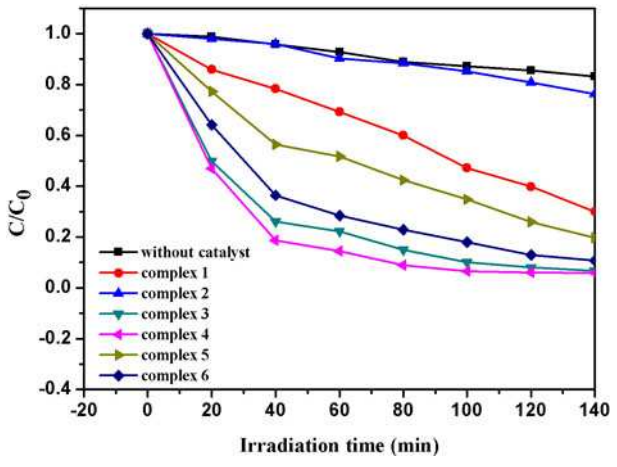

Figure 8. Photocatalytic decomposition of MB solution under UV light irradiation with the use of complexes **1**–**6** and the control experiment without any catalyst under the same conditions.

Although the optical band gap (Eg) was one key factor for the decomposition efficiency of the organic dyes, the structural characters of complexes also have important influences on their

photocatalytic activities. In this work, the band gaps of complexes **1**–**6** are 2.20, 2.17, 2.14, 2.08, 2.18, and 2.09 eV, respectively. Visibly, the band gaps of **1**, **2**, **3** and **5** are close to each other, while the band gap of **4** is also adjacent to that of **6**. However, their photocatalytic preformances are distinctively different, which could be influenced by the discrepancies of the complex structures[26-27], because of the small difference of optical band gap between each group of complexes ($\Delta Eg \leq 0.12$ eV). For instance, the band gap of **2** is astonishingly not the widest, but the degradation rate is the smallest, only 23.1 %. Herein, we tentatively surmise that it is possibly caused by the special structure of **2**. As described above, complex **2** is a 2-fold interpenetrating 3D architecture containing left- and right-handed helical chains, the pyknotic structure of which will be not conducive to the adsorption and desorption of O_2/hydroxyl (OH^-) on its surface and the transport of excited holes/electrons to its surface, to retard the formation of the hydroxyl radicals (·OH) and further impedes the occurrence of the catalytic reaction. Therefore, we speculate that the interpenetrating framework containing helical chains could be not good for starting the decomposition reaction.

Conclusions

To sum up, the synchronous use of the btbb and related carboxylate coligands to react with Cd(II) ions affords six complex architectures. These complexes exhibit appealing and enthralling structural motifs. The analysis of optical energy gaps of complexes **1**–**6** proves that these complexes are potential semiconductive materials. The photocatalytic behaviors of complexes **1**–**6** attest that **3**, **4** and **6** may be good photocatalysts for the photodegradation of MB.

Acknowledgments

We gratefully acknowledge financial support by the National Natural Science Foundation (Nos 21371155 and 21201152) and Research Found for the Doctoral Program of Higher Education of China (20124101110002).

References

1 (a) C. G. Daughton, *Environ. Impact Assess. Rev.,* 2004, **24**, 711; (b) M. Carballa, F. Omil, J. M. Lema, M. Llompart, C. García-Jares, I. Rodríguez, M. Gó mez and T. Ternes, *Water Res.,* 2004, **38**, 2918; (c) Y. Wu, D. N. Lerner, S. A Banwart, S. F. Thornton and R. W. Pickup, *J. Environ. Qual.,* 2006, **35**, 2021; (d) S. K. Khetan and T. J. Collins, *Chem. Rev.,* 2007, **107**, 2319; (e) C. Y. Sun, D. Zhao, C. C. Chen, W. H. Ma and J. C. Zhao, *Environ. Sci. Technol.,* 2009, **43**, 157; (f) C. Y. Sun, C. C. Chen, W. H. Ma and J. C. Zhao, *Phys. Chem. Chem. Phys.,* 2011, **13**, 1957.

2 (a) J. O. Nriagu and J. M. Pacyna, *Nature,* 1988, **333**, 134; (b) S. K. Li, F. Z. Huang, Y. Wang, Y. H. Shen, L. G. Qiu, A. J. Xie and S. J. Xu, *J. Mater. Chem.,* 2011, **21**, 7459.

3 R. Ganesh, G. D. Boardman and D. Michelson, *Water Res.,* 1994, **28**, 1367.

4 Z. X. Shu, X. L. Jiao and D. R. Chen, *CrystEngComm,* 2013, **15**, 4288.

5 (a) M. Alvaro, E. Carbonell, B. Ferrer, F. X. Llabrés i Xamena and H. Garcia, *Chem.–Eur. J.,* 2007, **13**, 5106; (b) Z. L. Liao, G. D. Li, M. H. Bi and J. S. Chen, *Inorg. Chem.,* 2008, **47**, 4844; (c) Z. T. Yu, Z. L. Liao, Y. S. Jiang, G. H. Li, G. D. Li and J. S. Chen, *Chem. Commun.,* 2004, 1814; (d) Z. T. Yu, Z. L. Liao, Y. S. Jiang, G. H. Li and J. S. Chen, *Chem.–Eur. J.,* 2005, **11**, 2642; (e) P. Mahata, G. Madras and S. Natarajan, *Catal. Lett.,* 2007, **115**, 27; (f) J. H. Choi, Y. J. Choi, J. W. Lee, W. H. Shin and J. K. Kang, *Phys. Chem. Chem. Phys.,* 2009, **11**, 628.

6 (a) P. Mahata, G. Madras and S. Natarajan, *J. Phys. Chem. B,* 2006, **110**, 13759; (b) C. G. Silva, A. Corma and H. Garcia, *J. Mater. Chem.,* 2010, **20**, 3141; (c) T. Tachikawa, J. R. Choi, M. Fujitsuka and T. Majima, *J. Phys. Chem. C,* 2008, **112**, 14090; (d) L. L. Wen, F. Wang, J. Feng, K. L. Lv, C. G. Wang and D. F. Li, *Cryst. Growth Des.,* 2009, **9**, 3581; (e) J. X. Meng, Y. G. Li, H. Fu, X. L. Wang and E. B. Wang, *CrystEngComm,* 2011, **13**, 649; (f) J. X. Meng, Y. Lu, Y. G. Li, H. Fu and E. B. Wang, *CrystEngComm,* 2011, **13**, 2479.

7 (a) O. D. Friedrichs, M. O'Keeffe, O. M. Yaghi, *Acta Crystallogr. A,* 2003, **59**, 22; (b) O. D. Friedrichs, M. O'Keeffe, O. M. Yaghi, *Acta Crystallogr. A,* 2003, **59**, 515; (c) Y. Qi, F. Luo, Y. X. Che, J. M. Zheng, *Cryst. Growth Des.* 2008, **8**, 606.

8 (a) M. L. Tong, B. H. Ye, J. W. Cai, X. M. Chen, S. W. Ng, *Inorg.Chem.,* 1998, **37**, 2645; (b) T. L. Hennigar, D. C. MacQuarrie, P. Losier, R. D. Rogers, M. J. Zaworoko, *Angew. Chem., Int. Ed. Engl.* 1997, **36**, 972; (c) W. L. Zhang, Y. Y. Liu, J. F. Ma, H. Jiang, J. Yang, G. J. Ping, *Cryst. Growth Des.,* 2008, **8**, 1250; (d) J. Fan, G. T. Yee, G. B. Wang, B. E. Hanson, *Inorg.Chem.,* 2006, **45**, 599; (e) S. L. James, *Chem. Soc. Rev.*, 2003, **32**, 276; (f) S. L. Huang, L. H. Weng, G. X. Jin, Dalton Trans., 2012, **41**, 11657.

9 (a) J. S. Hu, Y. J. Shang, X. Q. Yao, L. Qin, Y. Z. Li, Z. J. Guo, H. G. Zheng, Z. L. Xue, *Cryst. Growth Des.,* 2010, **10**, 4135; (b) X. Q. Yao, D. P. Cao, J. S. Hu, Y. Z. Li, Z. J. Guo, H. G. Zheng, *Cryst. Growth Des.,* 2011, **11**, 231; (c) S. Q. Zang, M. M. Dong, Y. J. Fan, H. W. Hou, T. C. W. Mak, *Cryst. Growth Des.,* 2012, **12**, 1239; (d) H. A. Habib, J. Sanchiz, C. Janiak, *Inorg. Chim. Acta.,* 2009, **362**, 2452; (e) H.A. Habib, J. Sanchiz , C. Janiak, *Dalton Trans.,* 2008, 1734; (f) B. Wisser, Y. R. Lu, C. Janiak, *Z. Anorg. Allg. Chem.,* 2007, **633**, 1189.

10 (a) M. Du, X. J. Jiang, X. J. Zhao, Inorg. Chem., 2006, **45**, 3998; (b) J. C. Jin, Y. N. Zhang, Y. Y. Wang, J. Q. Liu, Z. Dong, Q. Z. Shi, *Chem. Asian J.,* 2010, **5**1, 611; (c) E. C. Yang, Z. Y. Liu, X. J. Shi, Q. Q. Liang, X. J. Zhao, *Inorg. Chem.,* 2010, **49**, 7969; (d) J. Xu, Z. R. Pan, T. W. Wang, Y. Z. Li, Z. J. Guo, S. R. Batten, H. G. Zheng, *CrystEngComm.,* 2010, **12**, 612; (e) S. L. Huang, Y. J. Lin, T. S. Andy Hor, G. X. Jin, *J. Am. Chem. Soc.* 2013, **135**, 8125.

11 (a) Y. Gong, Z. Hao, J. L. Sun, H. F. Shi, P. G. Jiang and J. H. Lin, *Dalton Trans.,* 2013, **42**, 13241; (b) X. L. Wang, J. J. Huang, L. L. Liu, G. C. Liu, H. Y. Lin, J. W. Zhang, N. L. Chen and Y. Qu, *CrystEngComm.,* 2013, **15**, 1960; (c) Y. Gong, T. Wua and J. H. Lin, *CrystEngComm.,* 2012, **14**, 3727.

12 (a) J. Wu, Y. L. Song, E. P. Zhang, H. W. Hou, Y. T. Fan and Y. Zhu, *Chem. Eur. J.,* 2006, **12**, 5823; (b) W. Li, H. P. Jia, Z. F. Ju and J. Zhang, *Cryst. Growth Des.,* 2006, **6**, 2136; (c) Y. Liu, G. Li, X. Li and Y. Cui, *Angew. Chem. Int. Ed.,* 2007, **46**, 6301; (d) H. W. Hou, X. R. Meng, Y. L. Song, Y. T. Fan, Y. Zhu, H. J. Lu, C. X. Du and W. H. Shao *Inorg. Chem.*, 2002, **41**, 4068; (e) L. Wang, M. Yang, G. H. Li, Z. Shi and S. H. Feng *Inorg. Chem.*, 2006, **45**, 2474; (f) J. D. Lin, X. F. Long, P. Lin and S. W. Du, *Cryst. Growth Des.,* 2010, **10**, 146.

13 (a) P. Cui, Z. Chen, D. L. Gao, B. Zhao, W. Shi and P. Cheng, *Cryst. Growth Des.,* 2010, **10**, 4370; (b) L. N. Li, S. Y. Wang, T. L. Chen, Z. H. Sun, J. H. Luo and M. C. Hong, *Cryst. Growth Des.,* 2012, **12**, 4109; (c) X. L. Wang, Y. F. Bi, H. Y. Lin and G. C. Liu, *Cryst. Growth Des.,* 2007, **7**, 1086; (d) J. C. Dai, X. T. Wu, Z. Y. Fu, C. P. Cui, S. M. Hu, W. X. Du, L. M. Wu, H. H. Zhang, R. Q. Sun, *Inorg. Chem.,* 2002, **41**, 1391; (e) H. A. Habib, A. Hoffmann, H. A. Hoppea, C. Janiak, *Dalton Trans.,* 2009, 1742; (f) D. Sun, L. L. Han, S. Yuan, Y. K. Deng, M. Z. Xu and D. F. Sun, *Cryst. Growth Des.,* 2013, **13**, 377.

14 (a) B. H. Ye, B. B. Ding, Y. Q. Weng, X. M. Chen, *Cryst. Growth Des.,* 2005, **5**, 801; (b) Y. Qi, Y. X. Che, J. M. Zheng, *Cryst. Growth Des.,* 2008, **8**, 3602; (c) S. R. Zhu, H. Zhang, Y. M. Zhao, M. Shao, Z. X. Wang, M. X. Li, *J. Mol. Struct.,* 2008, **892**, 420; (d) Z. Su, J. Xu, J. Fan, D. J. Liu, Q. Chu, M. S. Chen, S. S. Chen, G. X. Liu, X. F. Wang, W. Y. Sun, *Cryst. Growth Des.,* 2009, **9**, 2801; (e) M. Du, X. J. Jiang, X. J. Zhao, *Inorg. Chem.,* 2007, **46**, 3984.

15 (a) K. M. Ok, D. O'Hare, *Dalton Trans.,* 2008, 5560; (b) S. Ma, J. M. Simmons, D. Yuan, J. R. Li, W. Weng, D. J. Liua, H. C. Zhou, *Chem. Commun.,* 2009, 4049; (c) B. Zheng, J. Bai, J. Duan, L. Wojtas, M. J.

Zaworotko, *J. Am. Chem. Soc.,* 2011, **133**, 748; (d) B. H. Ye, M. L. Tong, X. M. Chen, *Coord. Chem. Rev.,* 2005, **249**, 545; (e) D. R. Xiao, E. B. Wang, H. Y. An, Y. G. Li, Z. M. Su, C. Y. Sun, *Chem. Eur. J.,* 2006, **12**, 6528; (f) Y. B. Men, J. L. Sun, Z. T. Huang, Q. Y. Zheng, *Angew. Chem., Int. Ed.,* 2009, **48**, 2873; (g) S. Q. Zang, R. Liang, Y. J. Fan, H. W. Hou, T. C. W. Mak, *Dalton Trans.,* 2010, 8022.

16 Bronisz, R. *Inorg. Chem.,* 2005, **44**, 4463.

17 G. M. Sheldrick, *Acta Crystallogr. A.,* 2008, **64**, 112.

18 X. J. Shi, X. Wang, L. K. Li, H. W. Hou and Y. T. Fan, *Cryst. Growth Des.,* 2010, **10**, 2490.

19 (a) J. X. Xu, R. Y. Wang, Y. M. Li, Z. Y. Gao, R. Yao, S. Wang and B. L. Wu, *Eur. J. Inorg. Chem.,* 2012, **20**, 3349; (b) X. J. Wang, Y. H. Liu, C. Y. Xu, Q. Q. Guo, H. W. Hou and Y. T. Fan, *Cryst. Growth Des.,* 2012, **12**, 2435; (c) L. Y. Zhang, J. P. Zhang, Y. Y. Lin and X. M. Chen, *Cryst. Growth Des.,* 2006, **6**, 1684; (d) Q. Shi, Y. T. Sun, L. Z. Sheng, K. F. Ma, M. L. Hu, X. G. Hu and S. M. Huang, *Cryst. Growth Des.,* 2008, **8**, 3401; (e) R. B. Zhang, Z. J. Li, Y. Y. Qin, J. K. Cheng, J. Zhang and Y. G. Yao, *Inorg. Chem.,* 2008, **47**, 4861; (f) Y. H. He, Y. L. Feng, Y. Z. Lan and Y. H. Wen, *Cryst. Growth Des.,* 2008, **8**, 3586.

20 Y. Gong, J. Li, J. B. Qin, T. Wu, R. Cao, J. H Li, *Cryst. Growth Des.* 2011, **11**, 1662.

21 (a) D. D. Censo, S. Fantacci, F. D. Angelis, C. Klein, N. Evans, K. Kalyanasundaram, H. J. Bolink, M. Grätzel, M. K. Nazeeruddin, *Inorg. Chem.,* 2008, **47**, 980; (b) S. Ohkoshi, H. Tokoro, T. Hozumi, Y. Zhang, K. Hashimoto, C. Mathonière, I. Bord, G. Rombaut, M. Verelst, C. C Moulin and F. Villain, *J. Am. Chem. Soc.,* 2006, **128**, 270; (c) J. H. Wang, Y. Q. Fang, L. Bourget-Merle, M. I. J. Polson, G. S. Hanan, A. Juris, F. Loiseau, S. Campagna, *Chem. Eur. J.,* 2006, **12**, 8539; (d) M. Stadler, F. Puntoriero, S. Campagna, N. Kyritsakas, R. Welter, J. M. Lehn, *Chem. Eur. J.,* 2005, **11**, 3997.

22 (a) S. C. Rasmussen, R. L. Schwiderski and M. E. Mulholland, *Chem. Commun.,* 2011, **47**, 11394; (b) F. Wang, Z. S. Liu, H. Yang, Y. X. Tan and J. Zhang, *Angew. Chem. Int. Ed.,* 2011, **50**, 450.

23 (a) A. K. Paul, G. Madras and S. Natarajan, *Phys. Chem. Chem. Phys.,* 2009, **11**, 11285; (b) G. S. Yang, H. Y. Zang, Y. Q. Lan, X. L. Wang, C. J. Jiang, Z. M. Su and L. D. Zhu, *CrystEngComm.,* 2011, **13**, 1461.

24 (a) J. Guo, J. F. Ma, B. Liu, W. Q. Kan, J. Yang, *Cryst. Growth Des.,* 2011, **11**, 3609; (b) H. S. Liu, Y. Q. Lan, S. L. Li, *Cryst. Growth Des.,* 2010, **10**, 5221.

25 (a) M. Alvaro, E. Carbonell, B. Ferrer, F. X. Llabres i Xamena and H. Garcia, *Chem.–Eur. J.,* 2007, **13**, 5106; (b) Z. L. Liao, G. D. Li, M. H. Bi and J. S. Chen, *Inorg. Chem.,* 2008, **47**, 4844; (c) Z. T. Yu, Z. L. Liao, Y. S. Jiang, G. H. Li, G. D. Li and J. S. Chen, *Chem. Commun.,* 2004, 1814; (d) Z. T. Yu, Z. L. Liao, Y. S. Jiang, G. H. Li and J. S. Chen, *Chem.–Eur. J.,* 2005, **11**, 2642; (e) H. S. Lin and P. A. Maggard, *Inorg. Chem.,* 2008, **47**, 8044; (f) P. Mahata, G. Madras and S. Natarajan, *Catal. Lett.,* 2007, **115**, 27.

26 (a) B. Liu, Z. T. Yu, J. Yang, H. Wu, Y. Y. Liu and J. F. Ma, *Inorg. Chem.,* 2011, **50**, 8967; (b) Y. Hu, F. Luo and F. F. Dong, *Chem. Commun.,* 2011, **47**, 761; (c) W. Q. Kan, B. Liu, J. Yang, Y. Y. Liu and J. F. Ma, *Cryst. Growth Des.,* 2012, **12**, 2288; (d) H. Fu, Y. G. Li, Y. Lu, W. L. Chen, Q. Wu, J. X. Meng, X. L. Wang, Z. M. Zhang and E. B. Wang, *Cryst. Growth Des.,* 2011, **11**, 458; (e) Q. Wu, W. L. Chen, D. Liu, C. Liang, Y. G. Li, S. W. Lin and E. Wang, *Dalton Trans.,* 2011, **40**, 56.

27 (a) M. Q. Hu and Y. M. Xu, *Chemosphere,* 2004, **54**, 431; (b) K. L. Lv and Y. M. Xu, *J. Phys. Chem. B,* 2006, **110**, 6204; (c) L. L. Wen, J. B. Zhao, K. L. Lv, Y. H. Wu, K. J. Deng, X. K. Leng and D. F. Li, *Cryst. Growth Des.,* 2012, **12**, 1603.

For Table of Contents Use Only

Structural Variability, Topological Analysis and Photocatalytic Properties of Neoteric Cd(II) Coordination Polymers Based on Semirigid Bis(Thiazolylbenzimidazole) and Different Types of Carboxylic Acid Linkers

Lu Liu, Jie Ding, Ming Li, Xiaofeng Lv, Jie Wu*, Hongwei Hou*, Yaoting Fan

Six charming architectures with differently structural and topological motifs have been obtained by introducing the carboxylate coligands into the system Cd(II)/btbb. The relatively narrow optical energy gaps of complexes **1**–**6** (< 2.30 eV) reflects their underlying semiconductive nature. Complexes **3**, **4** and **6** exhibit better photocatalytic activities in methylene blue (MB) degradation (**3**: 91.4 %, **4**: 92.7 %, **6**: 86.7 %, severally).

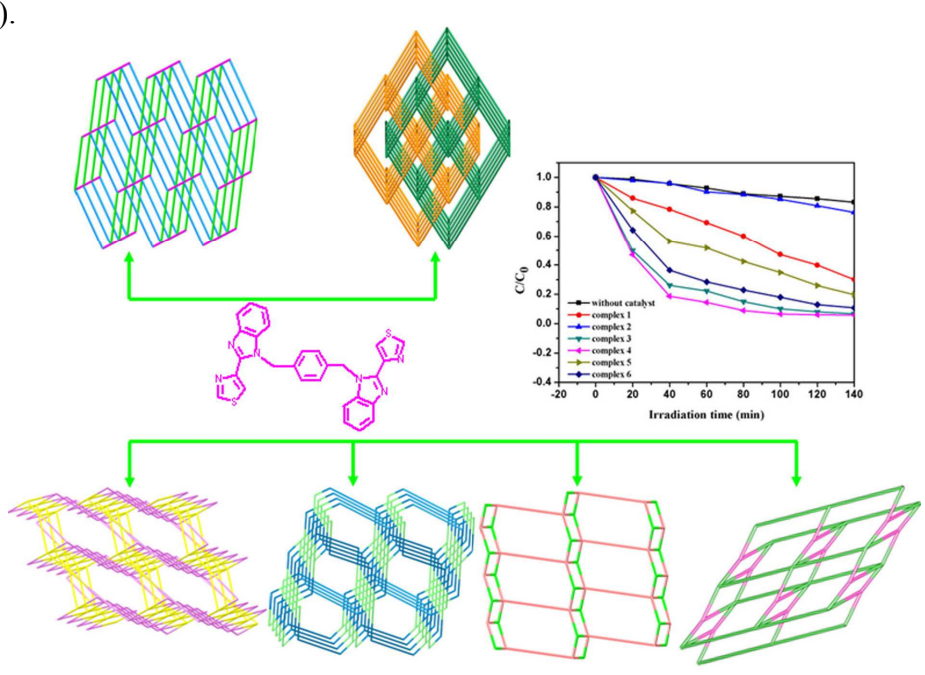

For Table of Contents Use Only

Structural Variability, Topological Analysis and Photocatalytic Properties of Neoteric Cd(II) Coordination Polymers Based on Semirigid Bis(Thiazolylbenzimidazole) and Different Types of Carboxylic Acid Linkers

Lu Liu, Jie Ding, Ming Li, Xiaofeng Lv, Jie Wu*, Hongwei Hou*, Yaoting Fan

Six charming architectures with differently structural and topological motifs have been obtained by introducing the carboxylate coligands into the system Cd(II)/btbb. The relatively narrow optical energy gaps of complexes **1**–**6** (< 2.30 eV) reflects their underlying semiconductive nature. Complexes **3**, **4** and **6** exhibit better photocatalytic activities in methylene blue (MB) degradation (**3**: 91.4 %, **4**: 92.7 %, **6**: 86.7 %, severally).